Phase-field simulations of solidification in binary and ternary systems using a finite element method

D. Danilov [a] and B. Nestler [b]

[a] *Institute of Applied Research, Karlsruhe University of Applied Sciences, Moltkestrasse 30, D-76133 Karlsruhe Germany*
[b] *Department of Computer Science, Karlsruhe University of Applied Sciences, Moltkestrasse 30, D-76133 Karlsruhe Germany*

Abstract

We present adaptive finite element simulations of dendritic and eutectic solidification in binary and ternary alloys. The computations are based on a recently formulated phase-field model that is especially appropriate for modelling non-isothermal solidification in multicomponent multiphase systems. In this approach, a set of governing equations for the phase-field variables, for the concentrations of the alloy components and for the temperature has to be solved numerically, ensuring local entropy production and the conservation of mass and inner energy. To efficiently perform numerical simulations, we developed a numerical scheme to solve the governing equations using a finite element method on an adaptive non-uniform mesh with highest resolution in the regions of the phase boundaries. Simulation results of the solidification in ternary $Ni_{60}Cu_{40-x}Cr_x$ alloys are presented investigating the influence of the alloy composition on the growth morphology and on the growth velocity. A morphology diagram is obtained that shows a transition from a dendritic to a globular structure with increasing Cr concentrations. Furthermore, we comment on 2D and 3D simulations of binary eutectic phase transformations. Regular oscillatory growth structures are observed combined with a topological change of the matrix phase in 3D. An outlook for the application of our methods to describe AlCu eutectics is given.

Key words: A1. Computer simulation, A1. Dendrites, A1. Eutectics, A1. Morphological stability, A1. Solidification, B1. Alloys.
PACS: : 64.70.Dv, 81.10.Aj, 81.30.Fb.

1. Introduction

Multicomponent alloys form the most important class of metallic materials for technical and industrial processes. Combined with the number of components is a wealth of different phases, phase transformations, complex thermodynamic interactions and pattern formations. The complex phase diagrams of multicomponent alloys show a variety of different solidification processes such as eutectic, peritectic and monotectic types of reaction. Since the most common solidification microstructures occuring in industrial alloys, such as Al and Fe based alloys, are dendrites and eutectic composite structures, we will concentrate our investi-

Email addresses: denis.danilov@fh-karlsruhe.de (D. Danilov), britta.nestler@fh-karlsruhe.de (B. Nestler).

gations on these two types of structures.

The phase-field modelling technique has made a significant progress during the last decade in simulating complex microstructures, such as dendritic and eutectic growth; see e.g. [1,2]. The newly introduced variable $\phi(x,t)$ in these models indicates the physical state of a system at each point in space. Differing from sharp interface concepts, $\phi(x,t)$ has a smooth transition at the interfaces (phase boundaries). In the bulk phases, $\phi(x,t)$ takes on constant values, e.g. $\phi(x,t) = 0$ for the liquid and $\phi(x,t) = 1$ for the solid phase. The governing equations consist of parabolic partial differential equations for the evolution of the phase state coupled to mass and heat transport equations. They serve for performing simulations of complex growth morphologies without explicitly tracking the phase boundaries. In a recent article [3], the phase-field methodology has been generalized to the case of arbitrary numbers of N components and M phases in alloy systems by introducing a vector of concentrations $c = (c_1, \ldots, c_N)$ and a vector of phase-field variables $\phi = (\phi_1, \ldots, \phi_M)$.

For computations based on diffuse interface models, it is required that the spatial resolution of the numerical method must be greater than the thickness of the diffusive phase boundary layer. The interfacial thickness itself must be less than the characteristic scale of the growing microstructure. In this case, a non-uniform grid with adaptive refinement can dramatically reduce the use of computational resources against a uniform grid with the same spatial resolution. For these reasons, we use an adaptive finite element method for solving the governing equations of the new multicomponent phase-field model.

The present report is part of our intension to apply the phase-field model and the numerical method to simulate solidification processes in real alloys which are usually multicomponent. We present simulation results of ternary dendritic and of binary eutectic growth. In particular, the ternary $Ni_{60}Cu_{40-x}Cr_x$ alloy system is considered to investigate the influence of interplaying solute fields on the interface stability, on the growth velocity and on the characteristic type of morphology. By choosing the Ni-Cu-Cr system, we build upon the binary Ni-Cu system which has been explored by phase-field modelling (e.g. [4]) and by molecular dynamics simulations in several papers (e.g. [5]). Hence, physical parameters are relatively well established. For our application to eutectic solidification, we constructed a symmetric binary model phase diagram. Special emphasis is laid on a discussion of oscillatory growth structures.

2. Phase-field model

The phase-field model in [3] has been formulated in a thermodynamically consistent way and allows for an arbitrary number of phases and components. It is defined solely via bulk free energies of the individual phases, the surface energy densities of the interfaces, the diffusion and mobility coefficients and yields classical moving boundary problems in the sharp interface limit. The approach is based on an entropy density functional $S(e,c,\phi)$ of the form

$$S = \int_\Omega \left[s(e,c,\phi) - \left(\varepsilon a(\phi, \nabla\phi) + \frac{1}{\varepsilon} w(\phi) \right) \right] dx. \tag{1}$$

The bulk entropy density s depends on the internal energy e, on the concentrations of components $c = (c_i)_{i=1}^N$, and on the phase-field variable $\phi = (\phi_\alpha)_{\alpha=1}^M$. The thermodynamics of the interfaces is given by the second and third term in the integral of Eq. (1) and is determined by the gradient energy density $a(\phi, \nabla\phi)$, the multi well potential $w(\phi)$ and a small scale parameter ε related to the thickness of the interface. The gradient energy and the multi well potential depend on the surface energy density σ and its anisotropy can be taken into account using appropriate choices of $a(\phi, \nabla\phi)$. The variable ϕ_α with $0 \leqslant \phi_\alpha \leqslant 1$ denotes the local fraction of phase α. It is required that the concentrations and phase-field variables fulfill the constraints

$$\sum_{i=1}^N c_i = 1, \quad \sum_{\alpha=1}^M \phi_\alpha = 1. \tag{2}$$

The evolution equations for the phase fields are postulated as

$$\omega\varepsilon\partial_t\phi_\alpha = \varepsilon(\nabla a_{,\nabla\phi_\alpha} - a_{,\phi_\alpha}) - \frac{1}{\varepsilon} w_{,\phi_\alpha} - \frac{f_{,\phi_\alpha}}{T} - \lambda, \tag{3}$$

where $f(T, c, \phi)$ is the free energy density and λ is a Lagrange multiplier such that the constraint in Eq. (2) for phase fields is satisfied. The kinetic factor $\omega = \omega(\phi, \nabla\phi)$ describes anisotropic interface kinetics and is related to the kinetic coefficient μ of atomic attachment in the linear response function "growth velocity–interfacial undercooling" at a flat front.

Considering an ideal solution system, we define the free energy density as follows

$$f(c,\phi) = \sum_{i=1}^{N}\sum_{\alpha=1}^{M} c_i L_i^\alpha \frac{T - T_i^\alpha}{T_i^\alpha} h(\phi_\alpha) + \frac{RT}{v_m}\sum_{i=1}^{N} c_i \ln c_i, \tag{4}$$

where L_i^α and T_i^α are the latent heat and the melting temperature of the component i in the phase α, respectively. R is the gas constant, v_m is the molar volume and $h(\phi_\alpha)$ is a monotone function on the interval $[0, 1]$ satisfying $h(0) = 0$ and $h(1) = 1$. Additionally, we consider an isothermal approximation with the temperature T being constant.

Assuming that the mass fluxes are linear functions of the thermodynamic driving forces, i.e. chemical potentials in isothermal approximation, mass balance equations can be written as

$$\partial_t c_i = -\nabla\left(\sum_{j=1}^{N} L_{ij}(c,\phi)\nabla\frac{-\mu_j}{T}\right), \tag{5}$$

with chemical potentials $\mu_i = f_{,c_i}$ and mobility coefficients given by

$$L_{ij}(c,\phi) = \frac{v_m}{R} D_i c_i \left(\delta_{ij} - \frac{D_j c_j}{\sum_{k=1}^{3} D_k c_k}\right). \tag{6}$$

The form of Eq. (6) allows different values of the bare trace diffusion coefficients $D_i(\phi)$ for the different components i and satisfies the constraint for concentrations in Eq. (2).

The evolution Eqns. (3) and (5) are solved using a finite element method with Lagrange elements and linear test functions. For the time evolution, a semi-implicit formulation is discretized to achieve better numerical stability. We generate a non-uniform adaptive mesh having the highest order of spatial resolution in the vicinity of the solid–liquid interface where the gradients of phase fields and concentrations reach maximal values. The mesh structure is adopted in time according to the evolution of phase and concentration fields using a refinement criterion based on the phase-field and concentration gradients.

3. Dendritic growth in ternary alloys

By numerical simulations, we investigate how the change of the alloy composition influences the growth morphology for a given solidification condition. In particular, we fix the initial undercooling and choose a ternary $Ni_{60}Cu_{40-x}Cr_x$ alloy as a prototype for this study. To recover the corresponding solidus and liquidus lines of the binary Ni-Cu and Ni-Cr phase diagrams in the region of concentrations up to 40 at.% of Cu or Cr, the following physical parameters are used: Melting temperatures $T_{\mathrm{Ni}} = 1728$ K, $T_{\mathrm{Cu}} = 1358$ K, $\widetilde{T}_{\mathrm{Cr}} = 1465$ K; latent heats $L_{\mathrm{Ni}} = 2350$ J/cm^3, $L_{\mathrm{Cu}} = 1728$ J/cm^3, $\widetilde{L}_{\mathrm{Cr}} = 1493$ J/cm^3 and a molar volume $v_m = 7.42$ cm^3. Since we do not consider the complete eutectic Ni-Cr phase diagram, the values of the melting temperature and of the latent heat for Cr are not the real physical data, but adjustable parameters in order to recover the actual binary phase diagram in the given region of concentrations. They are marked by a tilde to emphasize this difference from the data for Ni and Cu. Applying these values leads to a partition coefficient $k_e = 0.843$, to a liquidus slope $m_e = -3.27$ K/at.%, and to a freezing range $\Delta T_0 = m_e(k_e - 1)/k_e c_\infty = 24$ K for binary $Ni_{60}Cu_{40}$. Similarly, we obtain $k_e = 0.905$, $m_e = -2.08$ K/at.%, and $\Delta T_0 = 8.7$ K for the binary $Ni_{60}Cr_{40}$ system and the corresponding equilibrium phase diagram.

We assume that both surface properties, the surface energy density σ and the kinetic coefficient μ do not depend on the alloy composition and have the values $\sigma = 0.37$ J/m^2 and $\mu = 3.3$ mm/(s K), refering to [4]. The anisotropy of the interface properties plays an important role in the selection of the operating state during dendritic growth. In this study, we use the values calculated from molecular dynamics simulations. In [5], the strength of the surface energy anisotropy is given as 0.023 and the strength for kinetic anisotropy as 0.169.

The diffusion coefficients in the melt are $D_{\mathrm{Ni}} =$

3.82×10^{-9} m^2/s [5], $D_{\mathrm{Cu}} = 3.32 \times 10^{-9}$ m^2/s [5] and $D_{\mathrm{Cr}} = 1.5 \times 10^{-9}$ m^2/s. The diffusion coefficients in the solid phase are set as an equal value 10^{-13} m^2/s for all components. The small length scale parameter ε in the entropy functional (Eq. (1)) is $\varepsilon = 0.1$ μm.

Using the physical parameters given above, we carried out a series of numerical computations for different alloy compositions varying from $Ni_{60}Cu_{36}Cr_4$ to $Ni_{60}Cu_4Cr_{36}$. The concentration of Ni was kept at 60 at.% and the initial undercooling was fixed at 20 K measured from the equilibrium liquidus line in the phase diagram at a given composition of the melt. A morphological transition from dendritic to globular growth occurs at a melt composition of about $Ni_{60}Cu_{20}Cr_{20}$. The left side of Fig. 1 shows the dendritic morphologies observed for Cr concentrations less than 20 at.%. The right side of the figure displays globular morphologies for Cr concentration crossing this threshold. The velocity of the dendritic/globular tip increases linearly from 1.19 cm/s to 3.24 cm/s with increasing the concentration of Cr. An analogous type of dendritic to globular morphology transition depending on the undercooling has been observed in numerical simulations of binary alloy solidification and is discussed in [6].

Qualitatively, such transitions can be expected by comparing the initial undercooling ΔT with the freezing range ΔT_0: For the binary $Ni_{60}Cu_{40}$ alloy, the undercooling $\Delta T = 20$ K is less than the freezing range $\Delta T_0 = 24$ K, whereas for the binary $Ni_{60}Cr_{40}$ system the undercooling $\Delta T = 20$ K is greater than $\Delta T_0 = 8.7$ K. Thus the morphology change is related to the transition from a two-phase region (above the solidus line) to a one-phase region (below the solidus) in correspondance with the phase diagram. Qualitative analysis of growth structures should take into account the kinetic effects of the solid-liquid interface as well as the surface tension acting as stabilizing factor and the diffusion properties of alloy components as destabilizing forces due to concentration gradients [7].

4. Simulation of binary eutectic growth in 2D and 3D

To simulate eutectic phase transitions in a binary A–B alloy, where two solid phases α and β grow into an undercooled melt, we have constructed a typical eutectic phase diagram via the method of common tangents. In our computations, we consider the widely observed phenomenon of regular oscillations along the solid-solid interface driven by the triple junctions (Fig. 2). The initial concentration of the melt is chosen at the eutectic composition $c_A = c_B = 0.5$, where the two solid phases grow with equal phase fractions. A transition from steady state lamellar growth to an oscillatory pattern formation is found for an increasing difference of the initially set up phase fraction. For a ratio of 1:3 between the initial phase fraction of solid α:β, lamellar growth is re-established. For ratios of 1:4 and 1:6, regular oscillations with a characteristic amplitude and wave length as in Fig. (2) can be observed, whereas for a ratio 1:7, the β phase overgrows the initially dominating α

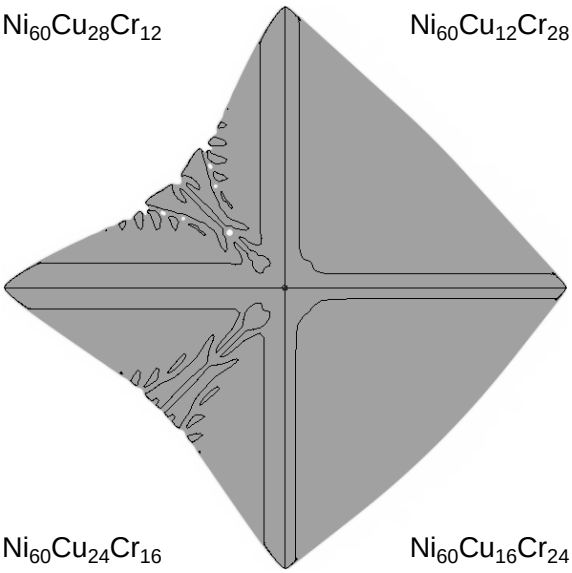

Fig. 1. Dendritic to globular morphological transition for different alloy compositions. The atomic percents of Cu and Cr are exchanged keeping Ni fixed at 60 at.%. The shaded regions correspond to the solid phase and the solid lines represent the isolines of average concentration of Ni in the solid phase.

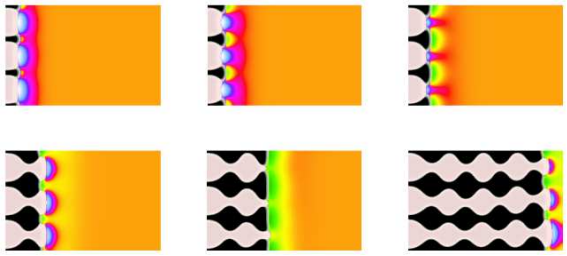

Fig. 2. Regular oscillations along the solid-solid interface during binary eutectic growth driven by the motion of the triple junction in 2D.

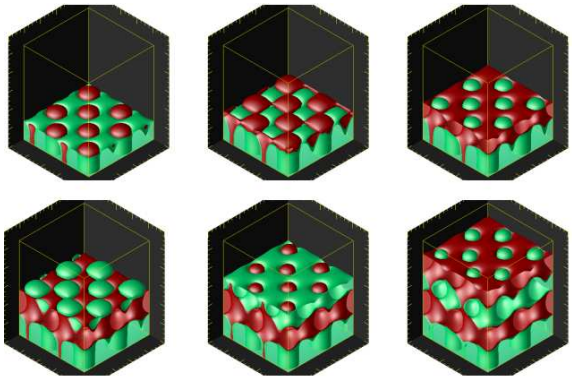

Fig. 3. Topological change of the microstructure with α rods embedded in a β matrix phase and visa versa. The formation results from regular 3D oscillations along the solid-solid interface.

solid phase. In such a case, a nucleation event takes place. Two-dimensional oscillatory structures have been discussed in [8] by boundary integral method and more recently in [9] by means of phase-field modelling.

The analogous type of oscillation can be observed for eutectic microstructure formations in three dimensions, Fig. 3. Performing an alternating topological change, α solid rods are embedded in a β matrix followed by the opposite situation of β crystals embedded in an α matrix. Further three-dimensional simulations of eutectic microstructures are reported in [10,11]

5. Conclusion

A new phase-field model for non-isothermal solidification in multicomponent multiphase alloy systems has been applied to ternary Ni-Cu-Cr primary phase growth and to binary eutectic growth of two solid phases into an undercooled melt. A transition from a dendritic to a globular structure is observed in our simulation series, while successively exchanging Cu by Cr. The experiences with a binary model eutectic will enable us to apply the modelling and simulation technique in eutectic and off-eutectic Al-Cu alloys in a forthcoming paper. Steady-state lamellar domains as well as different types of oscillations persisting over a wide range of compositions and growth rates are reported in [12].

The authors gratefully acknowledge helpful discussions with Mathis Plapp and the financial support provided by the German Research Foundation (DFG) under Grant No. Ne 882/2.

References

[1] B. Nestler and A. A. Wheeler, Physica D 138 (2000) 114.

[2] W.J. Boettinger, J.A. Warren, C. Beckermann, and A. Karma. Annu. Rev. Mater. Res. 32 (2002) 163.

[3] H. Garcke, B. Nestler, B. Stinner, SIAM J. Appl. Math. 64(3) (2004) 755.

[4] J. A. Warren, W. J. Boettinger, Acta metall. mater. 43(2) (1995) 689.

[5] J.J. Hoyt, M. Asta, A. Karma, Phys. Rev. Lett. 86 (24) (2001) 5530; J.J. Hoyt, B. Sadigh, M. Asta, S.M. Foiles, Acta mater. 47(11) (1999) 3181.

[6] P.K. Galenko, V.A. Zhuravlev. Physics of dendrites, World Scientific, Singapore, 1994.

[7] W. Kurz, D.J. Fisher, Fundamentals of Solidification, Trans Tech, Switzerland, 1998.

[8] A. Karma, A. Sarkissian, Met. Mat. Trans A 27 (1996) 635.

[9] W.T. Kim, T. Suzuki, M. Ode, J. Cryst. Growth 261 (2004) 135.

[10] M. Apel, B. Boettger, H.-J. Diepers, I. Steinbach, J. Cryst. Growth 237-239 (2002) 154.

[11] D. Lewis, T. Pusztai, L. Granasy, and J. Warren, JOM 56(4) (2004) 28.

[12] M. Zimmermann, A. Karma, M. Carrard. Phys. Rev. B. 42(1) (1990) 833.